A Systematic Design, Coordination, and Validation Framework for Directional Overcurrent Protection in Distribution Networks with Bidirectional Power Flow

S. Ntshiba[1*], S. Krishnamurthy[2], S. Nomandela[3]
[1,2]Department of Electrical, Electronic and Computer Engineering, Faculty of Engineering and the Built Environment, Cape Peninsula University of Technology, Bellville, P.O. Box 1906, Cape Town 7353, South Africa
[3]Department of Electrical Engineering, Faculty of Engineering, Built Environment and Information Technology, iYunivesithi Walter Sisulu, Buffalo City Campus, College Street, East London 5200, South Africa
[*]corresponding authors' emails: ntshibas@cput.ac.za

Abstract – *The increasing integration of distributed generation (DG) and renewable energy sources has fundamentally transformed traditional radial distribution networks into active systems with bidirectional power flow and variable fault-current levels. These changes reduce the effectiveness of conventional non-directional overcurrent protection schemes, particularly in maintaining selectivity and reliability. This study proposes a systematic approach to the design, coordination, and validation of a Directional Overcurrent Relay (DOCR) protection scheme for modern power systems. The proposed methodology is modeled and tested in DIgSILENT PowerFactory using the CIGRE Medium-Voltage/Low-Voltage (MV/LV) Test System. It evaluates directional Time-Overcurrent (TOC) relay characteristics across eight network topologies, including forward, reverse, and power-reversal fault scenarios. The scheme ensures accurate directional discrimination while maintaining a coordination margin of 0.3 seconds between primary and backup protection devices. Simulation results demonstrate that the coordinated DOCR scheme significantly improves fault selectivity, reduces fault-clearing times, and ensures reliable operation under varying system configurations. In grid-connected mode, single-phase-to-ground faults are cleared in approximately 0.256 to 1.034 seconds in line sections and between 0.99 and 1.1176 seconds at the busbar. Under islanded operation, fault-clearing times range from 0.28 to 0.834 seconds in line sections and from 1.398 to 1.593 seconds at the busbar. Overall, the findings confirm that properly coordinated DOCR schemes enhance protection performance in modern distribution networks. The study also identifies the need for future validation using larger distribution networks, additional fault types, AI-based adaptive protection techniques, real-time simulation, and hardware-in-the-loop (HIL) testing to further assess scalability and practical implementation.*

Keywords: *Directional overcurrent protection, distributed generation, distribution system, fault analysis, power system protection, protection coordination, relay coordination, smart grids*

Article History
Received 07 April 2026
Received in revised form 18 May 2026
Accepted 09 June 2026

I. Introduction

The integration of distributed generation (DG) and renewable energy sources, along with the transition to smart grid topologies, has complicated the protection of electrical distribution systems [1]. Traditional radial distribution networks with unidirectional power flow are evolving into active networks with bidirectional power flow, variable fault-current contributions, and dynamic operational topologies [2] - [3]. These changes fundamentally challenge traditional protection coordination techniques, which were developed for passive networks with predictable fault-current magnitudes and orientations [4]. Directional overcurrent relays (DOCRs) are the primary protection devices in distribution systems, providing fault detection and directional differentiation. The synchronization of these relays ensures selective fault isolation while maintaining system dependability and reducing customer interruptions [5] – [7].

The main problem addressed in this study is that conventional non-directional overcurrent protection schemes are not always suitable for distribution networks with DG, renewable energy sources, and possible islanded operation. In such systems, the magnitude and direction of

This is an Open Access article distributed under the terms of the Creative Commons Attribution-Noncommercial 3.0 Unported License, permitting copy and redistribution of the material and adaptation for commercial and uncommercial use.

fault current may vary with network topology, generation availability, and operating conditions. This may result in loss of selectivity, delayed tripping, unnecessary disconnection of healthy feeders, or failure of backup protection. Therefore, a systematic methodology is required to configure and validate DOCR settings under different operating conditions, especially where forward, reverse, and power-reversal fault-current scenarios may occur.

In recent years, extensive research has examined the influence of distributed generation penetration on power system protection [8] - [9]. In this research area, the literature review can be divided into two categories. The first category is the short-circuit analysis under the influence of distributed generation penetration in the power system. In [10], the study examines the transient short-circuit (SC) current behavior in future power systems with high penetration of non-synchronous generation (NSG). The work specifically evaluates how various factors influence SC current contributions from NSG employing fully rated converter technology. In addition, the study assesses the effect of different fault ride-through control strategies, developed in accordance with various grid code requirements, on the SC current response of NSG. The sensitivity of transient SC current to increasing levels of NSG penetration is further analyzed. The investigation is conducted through simulation studies, initially using a single-machine infinite-bus test system to provide a detailed assessment of the NSG SC response. The results are subsequently validated using the IEEE 9-bus test system under multiple NSG penetration scenarios implemented in DIgSILENT PowerFactory

Similarly, [11] developed four synthetic test networks across different voltage levels, designed to be representative and supported by non-confidential time-series data. Network development is based on extensive literature research on various grid parameters within the ENTSO-E interconnected European system, and these parameters are implemented in NEPLAN for network design. Load and generation profiles are incorporated to enable time-series analysis. The representativeness of the networks is validated through short-circuit analysis, with results compared against literature values for Austrian and German systems and against typical ranges for ENTSO-E grids. The findings indicate that the developed networks accurately reflect the behavior of European electrical networks and can be applied to assess technological impacts on ENTSO-E grids.

In [12], the paper investigates the impact of integrating DG units into an existing network on short-circuit current levels. The study compares the effects of installing a single centralized DG unit with installing multiple smaller distributed DG units with equivalent total capacity. The analysis is conducted using the IEEE 37-bus test system, simulated in DIgSILENT PowerFactory.

Building on the first category, some researchers have focused on the second category, which involves configuring protection systems based on short-circuit characteristics. Authors [13] proposed a standard overcurrent protection scheme for the CIGRE Task Force C06.04.02 European distribution networks, which are widely used in studies on distributed generation penetration. It establishes a common foundation for researchers investigating the integration of DG, enabling further analysis of protection system-related challenges. Similarly, [14] presented a concise definition of overcurrent protection settings for the CIGRE Medium-Voltage/Low-Voltage (MV/LV) Test System, which is widely recommended for studies of renewable-source penetration. The study provides detailed and educational calculations and results for both non-directional and directional overcurrent protection relays. The setting definitions account for multiple operating conditions, and two short-circuit types: three-phase and single-line-to-ground. The authors claim that the paper's key contribution is the validation of the overcurrent protection settings for the CIGRE MV/LV Test System, suitable for teaching and research applications.

While [15] examines the protection system of a German 20 kV distribution network, focusing on fault-clearing times under variable short-circuit conditions. An automated protection security assessment tool is employed for the analysis. Initially, fault-clearing times are determined across two protection zones in the existing grid without DG infeed. Two scenarios are considered: first, with the sub-transmission network short-circuited, with short-circuit power reduced to 70%. Furthermore, the authors recommended that future research consider DG behavior during faults. Additionally, a more detailed investigation of loosely coupled devices, including fuses, relays, back-to-back stations, and fault current limiters, is required.

In [16], a methodology for designing protection systems was proposed, focusing on configuring directional overcurrent protection settings and providing detailed implementation guidance. The methodology is tested and validated on the well-known CIGRE MV/LV Test System using DIgSILENT PowerFactory version 2023 SP1. The authors suggested that real-time simulations and hardware-in-the-loop (HIL) testing could be employed in future research. Additionally, applying this methodology to a larger test system may greatly enhance wide-area monitoring, control, and protection capabilities in future power networks.

The reviewed literature highlights a gap in the comprehensive overview of protection system configuration settings, emphasizing the need for a systematic approach that can accommodate the increasing integration of DG in future electrical distribution systems. To address this, the paper presents a methodology for configuring protection systems that can adapt to dynamic changes in DG-integrated and islanded systems. Short-circuit analysis and overcurrent protection are used, and

the proposed system is validated using a relay model in the software to ensure accurate and reliable operation. The approach is validated using the CIGRE MV/LV Test System under various operating conditions.

The remainder of the article is divided into the following sections. Section II provides an overview of overcurrent protection with two features: non-directional and directional. Section III outlines the methodology for configuring the protection system in a step-by-step implementation. Section IV provides the network data. Section V presents the case study, including the test system description, the overcurrent protection design, and its configuration. Section VI presents the results and discussion of the proposed protection system. Finally, Section VII concludes this paper with a summary and suggestions for further studies.

II. Overcurrent protection fundamentals

Overcurrent protection remains one of the most widely used protection functions in electrical distribution systems due to its simplicity, effectiveness, and reliability in detecting faults. In distribution networks, abnormal operating conditions such as short circuits or equipment failures are typically accompanied by a significant increase in current magnitude. Overcurrent protection schemes are specifically designed to detect these abnormal current levels and initiate corrective action to isolate the affected section of the network, thereby preventing equipment damage, minimizing service interruptions, and maintaining overall system stability.

Overcurrent relays can generally be classified into two main categories based on their functional characteristics. The first category is non-directional overcurrent relays, which operate solely on current magnitude, independent of current direction. The second category is directional overcurrent relays, which incorporate an additional directional element that enables the relay to determine the direction of current flow relative to a reference voltage. This directional capability is particularly important in complex or interconnected networks where fault currents may originate from multiple sources or flow in multiple directions. Together, these two types of overcurrent relays provide flexible and effective protection solutions suitable for a wide range of distribution system configurations.

A. Non-directional overcurrent protection

Non-directional overcurrent relays are commonly used in radial distribution feeders, the most widely used distribution system type. In addition to comparing the flowing current against predefined settings, these relays are distinguished by their ability to coordinate operation based on time–current (I–t) characteristic curves.

For example, consider a system with a single source and parallel feeder lines, each protected by relays at both ends, as illustrated in Figs. 1(a) and 1(b). If a fault occurs midway along Line 1, as shown in Fig. 1(a), relays RA and RB should operate before RC and RD to maintain supply continuity, allowing Line 2 to remain in service. This coordination is achieved by setting RA and RB to operate faster than RC and RD. Likewise, if a fault occurs on Bus 2, as shown in Fig. 1(b), relays RA and RB must trip first, while RC and RD provide backup protection.

Fig. 1 illustrates typical overcurrent protection responses under non-directional and directional operating principles [16]. Figs. 1(a) and 1(b) show non-directional overcurrent protection in a system with parallel feeders. In these cases, relay operation depends solely on the current magnitude. Therefore, when the fault current exceeds the relay pickup setting, relays may operate even when the fault is outside their intended protection zone. This can reduce selectivity and may disconnect healthy sections of the network.

Figs. 1(c), 1(d), and 1(e) illustrate directional overcurrent protection in a double-source or interconnected network. In these cases, each relay evaluates both the magnitude and direction of the fault current. A relay operates only when the measured current exceeds the pickup setting and flows within the assigned forward operating direction. Relays exposed to reverse-direction current remain restrained. This improves selectivity by ensuring that only the relays associated with the faulted feeder or section operate, while healthy feeders remain energized.

The operating time of overcurrent protection can be coordinated with protection objectives and fault conditions. This coordination is typically achieved using three time–current characteristics: instantaneous operation; time-dependent operation, including definite-time and inverse-time characteristics; and a combination of instantaneous and time-dependent functions. The operating time for inverse-time characteristics can be expressed as defined by IEC 60255 and IEEE C37.112 [17] - [18] and is given in Equation (1).

$$T_p = TMS \times \frac{\beta}{\left(\frac{I_f}{I_p}\right)^{\alpha} - 1} \qquad (1)$$

where $T_p$is the operating time of a relay, $TMS$is the time multiplier setting, $I_f$is the current detected by the relay, $I_p$is the relay pick-up current, and $\alpha$and $\beta$are slope constants.

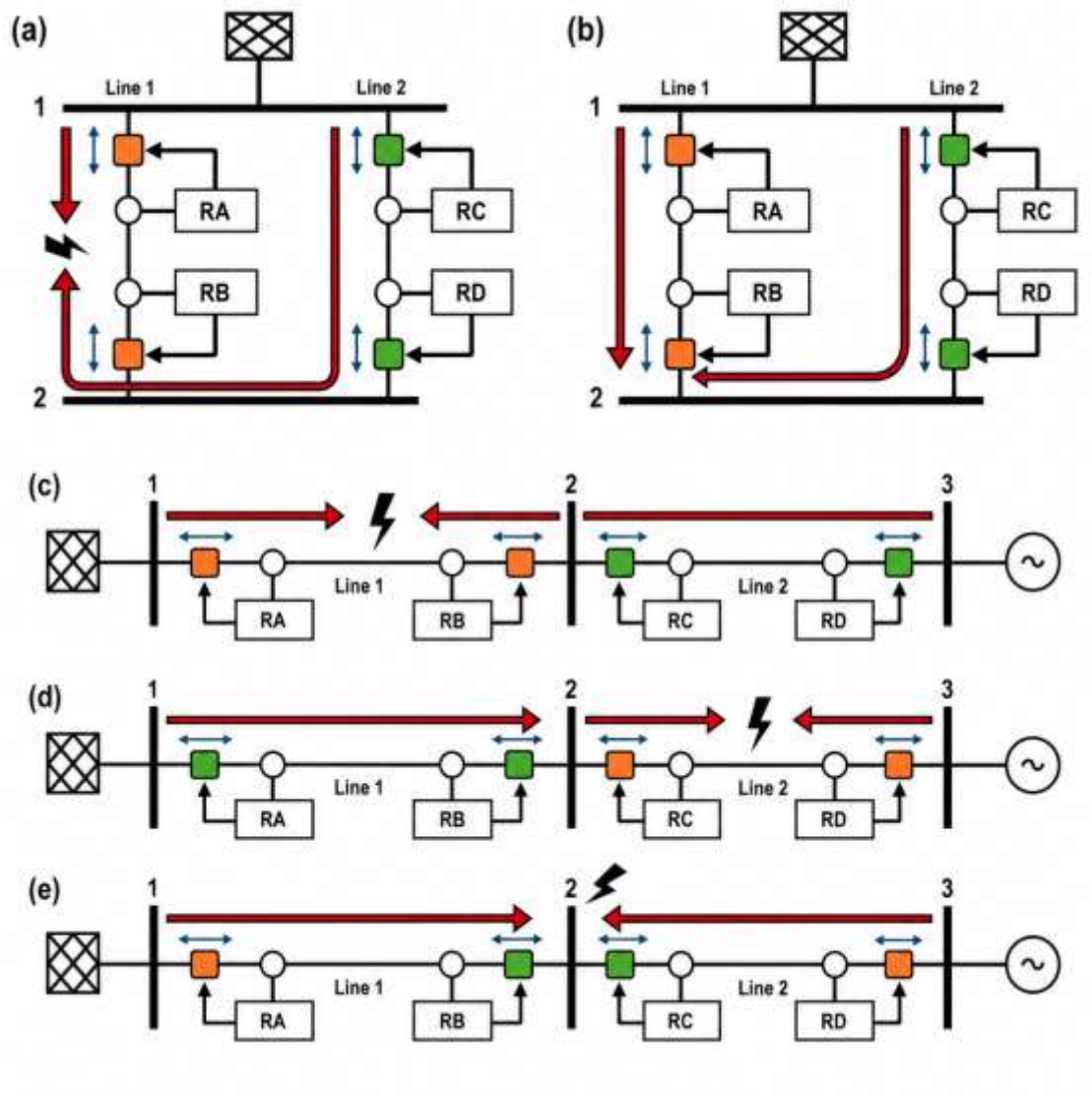


Fig. 1. Typical overcurrent protection in a power system [16]

B. Directional overcurrent protection

A directional overcurrent protection relay builds upon the basic principles of a non-directional overcurrent relay by incorporating an additional feature that allows it to distinguish the direction of the fault current. This means that the relay can be set to operate only for faults occurring in a specified direction, either forward or reverse, thereby improving selectivity and coordination within the protection scheme. This concept is illustrated in Fig. 2 [16].

The directional overcurrent relay is widely used in power systems where fault current may flow from multiple sources. As illustrated in Figs. 1(c)–1(e), a double-end-fed system is considered, with relays placed at both ends of the protected line. If a fault occurs in the middle of Line 1, as shown in Fig. 1(c), fault current flows from both sources towards the fault point. Relay RA operates according to its overcurrent setting, while relay RB operates only when the current flows in its preset forward direction. In this case, relay RB can operate because the current direction matches its directional setting.

Similarly, in Fig. 1(d), relays RC and RD can detect the fault current depending on their location and directional settings. However, if a fault occurs at Bus 2, as shown in Fig. 1(e), relays RB and RC do not operate because their preset directions do not correspond with the fault-current direction. Therefore, setting the direction of overcurrent protection in different fault scenarios is extremely important, especially in distribution networks with distributed generation, interconnected feeders, or bidirectional power flow.

The directional decision of the relay can be made using the relay characteristic angle, which is also known as the maximum torque angle, together with the polarising voltage, as shown in Fig. 3 [16]. This angle defines the relay operating sectors and separates the forward and

reverse zones. By evaluating the phase angle between the operating current and the polarising voltage, the relay determines whether the measured current falls within the predetermined forward or reverse region specified by the relay characteristic angle. This enables or disables the directional trip decision.

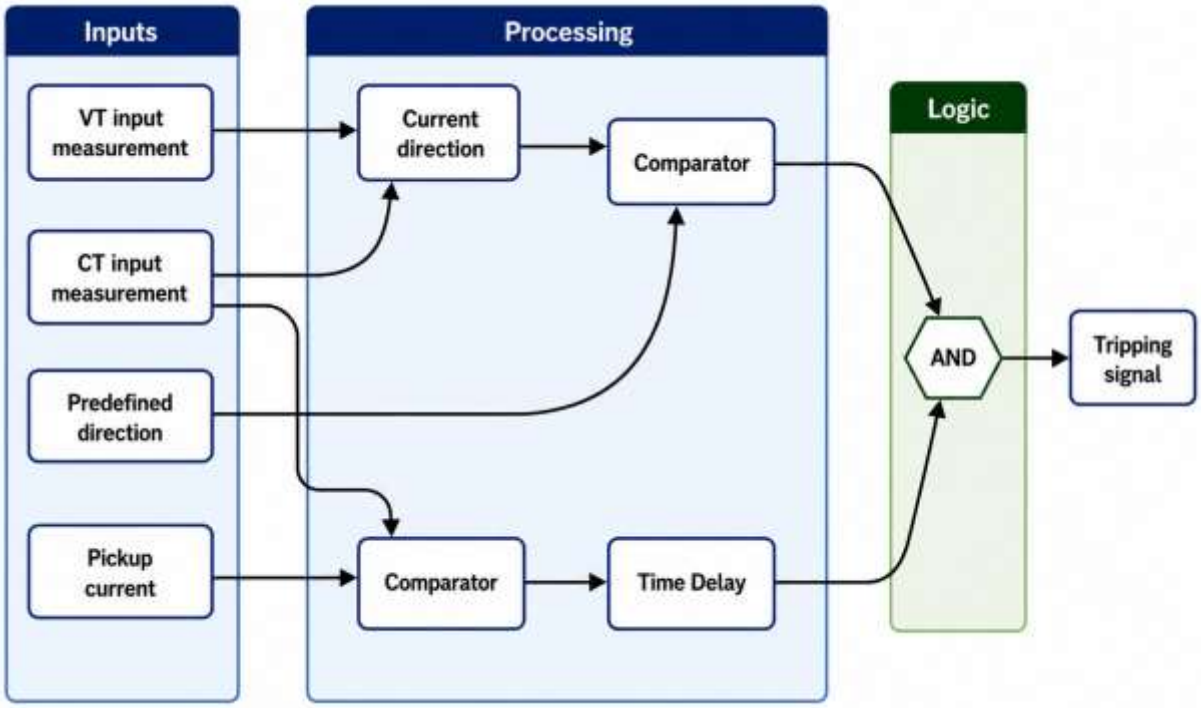


Fig. 2. Directional overcurrent protection block diagram [16]

Fig. 3 illustrates the phasor representation of the operating principle of a directional overcurrent relay. It shows how the relay distinguishes between forward and reverse fault-current conditions based on the phase relationship between current and voltage [16]. Fig. 3 also presents the polarising voltage as the reference phasor, typically drawn along the horizontal axis, while the operating current is shown as a rotating phasor. The relay determines its operating decision by evaluating the angular position of the operating current relative to the polarising voltage and the relay characteristic angle.

The characteristic angle is the relay setting that aligns the relay's sensitivity with the expected fault-current angle under the system's operating conditions. The maximum torque line, shown offset from the polarising voltage by the characteristic angle, indicates the direction at which the relay develops maximum operating torque and is therefore most sensitive to faults.

The zero-torque line represents the boundary between operating and restraining regions, where the relay produces no net operating torque. When the operating current phasor lies within the forward zone, the relay produces positive torque and is permitted to operate, indicating that the fault is located in the protected forward direction. Conversely, when the operating current lies within the reverse zone, the relay produces restraining torque and is prevented from tripping, indicating that the fault is external or located in the reverse direction.

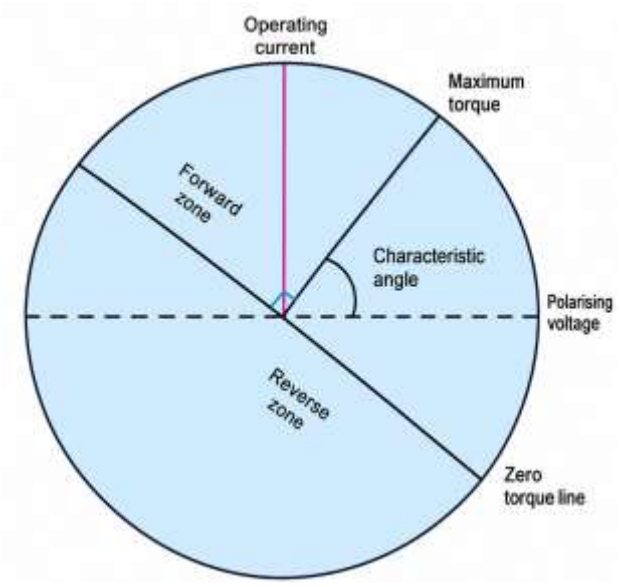


Fig. 3. Operating characteristics of a directional overcurrent relay [16]

This directional discrimination ensures that the relay operates selectively on faults within its designated protection zone while remaining stable under external faults or reverse power-flow conditions. The use of polarising voltage and characteristic angle settings allows the relay to maintain reliable directional detection even under varying system conditions, making directional

overcurrent protection highly suitable for interconnected and multi-source distribution networks.

III. Protection Design Methodology

The design of a directional overcurrent protection scheme requires a structured, systematic engineering approach to ensure reliable fault detection, proper coordination among protection devices, and secure system operation under both normal and abnormal operating conditions. The proposed methodology integrates system data analysis, relay setting calculations, directional-element configuration, coordination verification, and simulation validation. The following steps describe a comprehensive design methodology suitable for modern distribution networks, including multi-source and renewable-integrated systems.

Fig. 4 presents a structured methodology for configuring protection device settings within power system protection schemes. The authors propose that this methodology is versatile and can be effectively implemented across a wide range of protection technologies, including traditional protective devices, such as fuses, and more advanced systems, such as overcurrent and distance protection relays. The approach is intended to provide a systematic, standardized framework that supports protection engineers in achieving accurate, reliable, and coordinated protection settings across varying system operating conditions.

The research methodology steps 1 to 8 provided below involve developing a reliable power system protection scheme through a structured process. Initially, system data is collected and used to build an accurate network model for analysis. Fault studies are then conducted to determine system behavior under various fault conditions and to calculate fault levels. Based on these results, suitable relays are selected, and protection zones are defined to ensure proper coverage and selectivity. Current and voltage transformers are carefully chosen to provide accurate measurements to the relays. Overcurrent protection settings are then determined, followed by relay coordination to ensure the correct operation sequence between primary and backup devices. The scheme is further evaluated under bidirectional power flow conditions to account for the impact of distributed generation. Finally, simulations are performed to validate the overall performance of the protection system, ensuring it meets requirements for reliability, sensitivity, selectivity, and speed.

Step 1: Data collection and network modeling: Gather detailed electrical and operational data for the network under study. Accurate system modeling is essential for reliable protection design. Using this data, a network model is developed with simulation software or analytical tools to evaluate system behavior under fault conditions and during normal operation.

Step 2: Fault studies: Short-circuit studies are performed to determine the magnitude and distribution of fault currents throughout the network. This step ensures that relay settings are sufficiently sensitive to detect minimum fault currents while remaining stable under maximum load conditions. Both maximum and minimum fault-current scenarios must be evaluated to ensure reliable relay operation under all operating conditions.

Step 3: Relay selection and protection zones: Protection zones are defined to ensure complete network coverage with sufficient overlap between adjacent protection devices. Each relay is assigned a protection zone such that no part of the system remains unprotected. In this study, the relay at the line end (Ya) serves as the primary protection, while the relay at the line start (Xa) provides backup protection.

Step 4: current transformer (CT) and voltage transformer (VT) selection: The determination of CT and VT ratios follows directly from the system analysis conducted. For CT selection, the ratio must accommodate both the maximum anticipated load current and the prospective fault current magnitude. Critical to this selection is ensuring that the CT operates within its linear range during fault transients, thereby avoiding core saturation and ensuring reliable operation of the protection device. CTs were modeled to accurately measure feeder current for relay operation. In line with IEEE Std C37.110-1996 [19]. Similarly, the VT ratio is established based on the network's nominal and transient voltage levels, ensuring that secondary voltage quantities proportionally reflect primary system conditions in both normal and contingency operating states. This precise ratio selection underpins the metrological integrity required for dependable protection system performance.

Step 5: Overcurrent protection settings: The overcurrent element must be set to detect fault current while avoiding operation during normal or overload conditions. This includes the Pickup current setting, the Time dial, and the curve selection. The pickup current for the primary protection is set to 1.5 times the feeder load current. Protection settings are presented in Table VII.

Step 6: Relay coordination: Relay coordination ensures selective fault clearing, where the relay closest to the fault operates first, followed by backup protection if necessary. Typical coordination margins range between 0.2 s and 0.5 s, depending on system requirements [20]. In this study, 0.3 seconds are used.

Step 7: Verification under bidirectional power-flow conditions: Directional stability must be confirmed in all operating modes. This is to verify the relay performance under forward, reverse, and power-reversal fault conditions across different operational modes.

Step 8: Simulation and performance validation: The protection scheme is validated through dynamic fault simulation and sensitivity analysis. Simulation helps identify potential maloperations before field implementation. The protection systems must comply

with industry standards to ensure reliable operation under diverse faults and operating conditions. Validation typically employs offline and real-time simulation, as well as hardware-in-the-loop testing, to verify configuration performance.

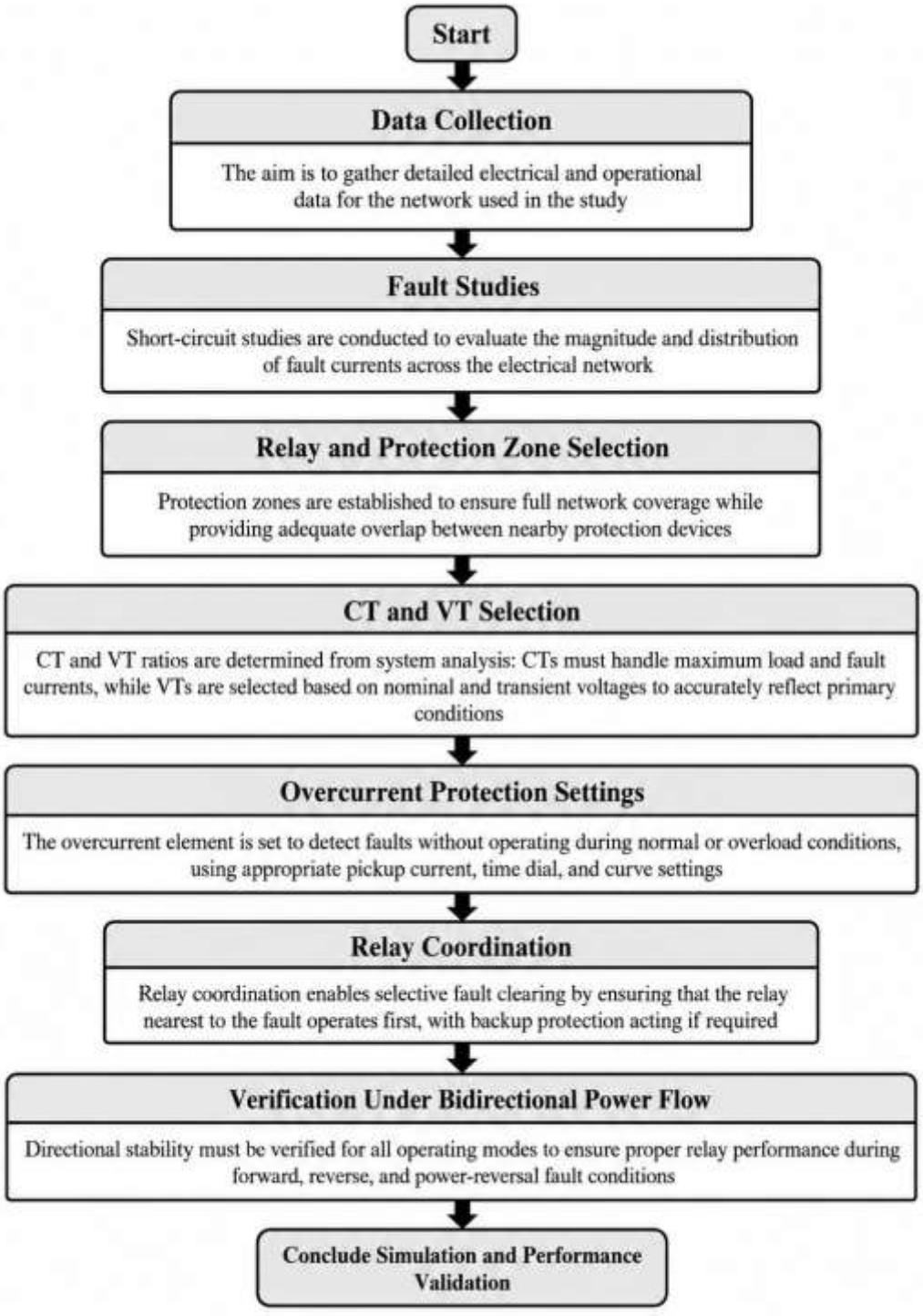


Fig.4. Protection system design methodology

For validation, the authors use offline simulation in DIgSILENT PowerFactory. The real-world SEL-351 relay from Schweitzer Engineering Laboratories (SEL) is selected to test the relay configuration. The validation study is implemented in Cases 1 and 8, which feature radial and interconnected topologies, respectively. Single-phase-to-ground faults are applied at the midpoint of Line 1–2 and at Bus 2 to evaluate the relay response under grid-connected and islanded operating conditions. It should be noted that in this paper, only single-phase-to-ground faults are presented. Although this fault type is suitable for demonstrating the proposed relay coordination and directional discrimination procedure, additional fault types, including three-phase, phase-to-phase, and double-line-to-ground faults, should be investigated in future studies to confirm the robustness of the framework under more severe fault conditions. This is supported by the literature, which indicates that most faults in distribution systems are single-phase-to-ground [21]. The detailed relay-characteristic plots and discussion of the relay operating sequence are presented in the Results and Discussion section.

IV. Modeled network data

This section presents the network data for the modeled electrical network shown in Fig. 5 in a structured and comprehensive manner.

The grid voltage levels and their corresponding voltage source parameters are outlined in Table I. Details pertaining to the five transformers, including their respective specifications, are summarized in Table II. The characteristics and operational parameters of the synchronous generators are provided in Table III. Furthermore, the transmission line parameters are presented systematically in Table IV, while the active and reactive power demands of the connected loads are documented in Table V.

Lastly, the protection settings are presented in Table VII.

TABLE I
VOLTAGE SOURCE PARAMETERS

DESCRIPTION	BUS TYPE	VOLTAGE	VOLTAGE SETPOINT	X/R RATIO
External grid	Slack bus	110 kV	1 PU	0.1

TABLE II
TRANSFORMER PARAMETERS

DESCRIPTION	SIZE (MVA)	VOLTAGE (KV)	VECTOR GROUP
TRF_01	25	110/20	Dyn1
TRF_12	25	110/20	Dyn1
TRF Conv_1	5	20/10.5	Dyn5
TRF Conv_2	5	20/10.5	Dyn5
TRF Conv_3	5	20/10.5	Dyn5

TABLE III
LINE PARAMETERS

DESCRIPTION	APPARENT POWER (MVA)	RATED VOLTAGE (KV)	POWER FACTOR	CONNECTION
Generators 1, to, and 3	4.855	10.5	0.8	YN

TABLE IV
LINE PARAMETERS

DESCRIPTION	RATED VOLTAGE (KV)	IMPEDANCE ($Z\angle\delta$)	IMPEDANCE ($Z = R + jX$)
L_1_2	20	$2.46\angle 55^{\circ}$	$1.41 + j2.02$
L_2_3	20	$3.86\angle 55^{\circ}$	$2.21 + j3.16$
L_3_4	20	$0.53\angle 55.02^{\circ}$	$0.31 + j0.44$
L_4_5	20	$0.49\angle 55.02^{\circ}$	$0.28 + j0.40$
L_5_6	20	$1.35\angle 55.02^{\circ}$	$0.77 + j1.10$
L_6_7	20	$0.21\angle 55.02^{\circ}$	$0.12 + j0.17$
L_7_8	20	$1.46\angle 55.02^{\circ}$	$0.84 + j1.20$
L_4_11	20	$0.43\angle 55.02^{\circ}$	$0.25 + j0.35$
L_10_11	20	$0.29\angle 55.02^{\circ}$	$0.17 + j0.24$
L_9_10	20	$0.67\angle 55.02^{\circ}$	$0.39 + j0.63$
L_8_9	20	$0.28\angle 55.02^{\circ}$	$0.16 + j0.23$
L_3_8	20	$1.14\angle 55.02^{\circ}$	$0.65 + j0.93$
L_8_14	20	$1.26\angle 35.67^{\circ}$	$1.02 + j0.73$
L_13_14	20	$1.88\angle 35.67^{\circ}$	$1.53 + j1.09$
L_12_13	20	$3.07\angle 35.67^{\circ}$	$2.49 + j1.79$

TABLE V
LOAD PARAMETERS

DESCRIPTION	ACTIVE POWER (MW)	POWER FACTOR
Load_1	1.2	0.96
Load_2	0.55	0.90
Load_3	0.445	0.97
Load_4	0.445	0.97
Load_5	0.75	0.97
Load_6	0.565	0.97
Load_7	0.09	0.85
Load_8	0.605	0.97
Load_9	0.675	0.85
Load_10	0.57	0.9
Load_10 (unbalanced condition)	0.38 (phase 1)	0.9
	0 (phase 2)	1.0
	0.19 (phase 3)	0.9
Load_11	0.34	0.97
Load_12	0.8	0.97
Load_13	0.04	0.85
Load_14	0.605	0.9

V. Case study

The study presented in this paper uses the CIGRE MV/LV Test System to evaluate the performance of the overcurrent protection system under two operating modes:

This is an Open Access article distributed under the terms of the Creative Commons Attribution-Noncommercial 3.0 Unported License, permitting copy and redistribution of the material and adaptation for commercial and uncommercial use.

grid-connected and islanded. CIGRE recommends this test system for investigating power system behavior under conditions of high renewable energy penetration [22].

The network topology can be configured using the available feeders and three isolation switches, S1, S2, and S3. More detailed information about this test system can be found in [22]. Additional variation can be introduced through eight operating cases, based on different configurations of switches S1, S2, and S3, as presented in Table VI.

When these switches are open, both feeders operate in a radial configuration. Closing switches S2 and S3 in Feeder 1 creates a loop or meshed configuration. Based on the position of switch S1, it can be assumed that the two feeders may be supplied either by the same substation or by different substations. Closing S1 interconnects the two feeders through a distribution line.

TABLE VI
OPERATING SCENARIOS ARE DEFINED BY SWITCH POSITIONS. SWITCH STATES: 0 = OPEN, 1 = CLOSED.

CASES	1	2	3	4	5	6	7	8
S1	0	0	0	0	1	1	1	1
S2	0	0	1	1	0	0	1	1
S3	0	1	0	1	0	1	0	1

These eight operating scenarios were selected to evaluate the proposed coordination framework under radial, looped, interconnected, grid-connected, and islanded operating conditions; however, the results remain specific to the CIGRE MV/LV Test System, and further validation on larger practical distribution systems is required to assess scalability.

TABLE VII
PROTECTION SYSTEM RELAY CONFIGURATION

GRID CONNECTED MODE					ISLANDED MODE				
Relay	**CT ratio**	**Branch Current (A)**	**Secondary Pick-up current (A)**	**Time dial**	**Relay**	**CT ratio**	**Branch Current (A)**	**Secondary Pick-up current (A)**	**Time Dial**
X1	200:1	130	0.98	0.36	X1	75:1	37	0.74	0.05
Y2	200:1	130	0.98	0.05	Y2	75:1	37	0.74	0.05
X2	200:1	130	0.98	0.3	X2	75:1	37	0.74	0.2
Y3	200:1	130	0.98	0.05	Y3	75:1	37	0.74	0.05
X3A	100:1	56	0.84	0.27	X3A	100:1	53	0.84	0.42
Y4	75:1	56	0.84	0.05	Y4	100:1	53	0.84	0.05
X4A	75:1	42	0.84	0.24	X4A	75:1	39	0.78	0.23
Y5	75:1	42	0.84	0.05	Y5	75:1	39	0.78	0.05
X5	50:1	18	0.54	0.05	X5	50:1	17	0.31	0.05
Y6	50:1	18	0.54	0.05	Y6	50:1	17	0.31	0.05
X8B	50:1	20	0.6	0.24	X8B	50:1	33	0.66	
X3B	100:1	57	0.86	0.27	X3B	100:1	53	0.84	0.42
Y8	100:1	57	0.86	0.05	Y8	100:1	53	0.84	0.05
X8A	75:1	35	0.7	0.24	X8A	50:1	33	0.66	0.38
Y9	75:1	35	0.7	0.05	Y9	50:1	33	0.66	0.05
X9	50:1	11	0.33	0.2	X9	50:1	11	0.33	0.22
Y10	50:1	11	0.33	0.05	Y10	50:1	11	0.33	0.05
X10	50:1	11	0.33	0.05	X10	50:1	11	0.33	0.05
Y11	50:1	11	0.33	0.05	Y11	50:1	11	0.33	0.05
X12	50:1	21	0.63	0.22	X12	-	-	-	-
Y13	50:1	21	0.63	0.05	Y13	50:1	20	0.6	0.05
X13	50:1	20	0.6	0.05	X13	-	-	-	-
Y14	50:1	20	0.6	0.05	Y14	50:1	25	0.75	0.2

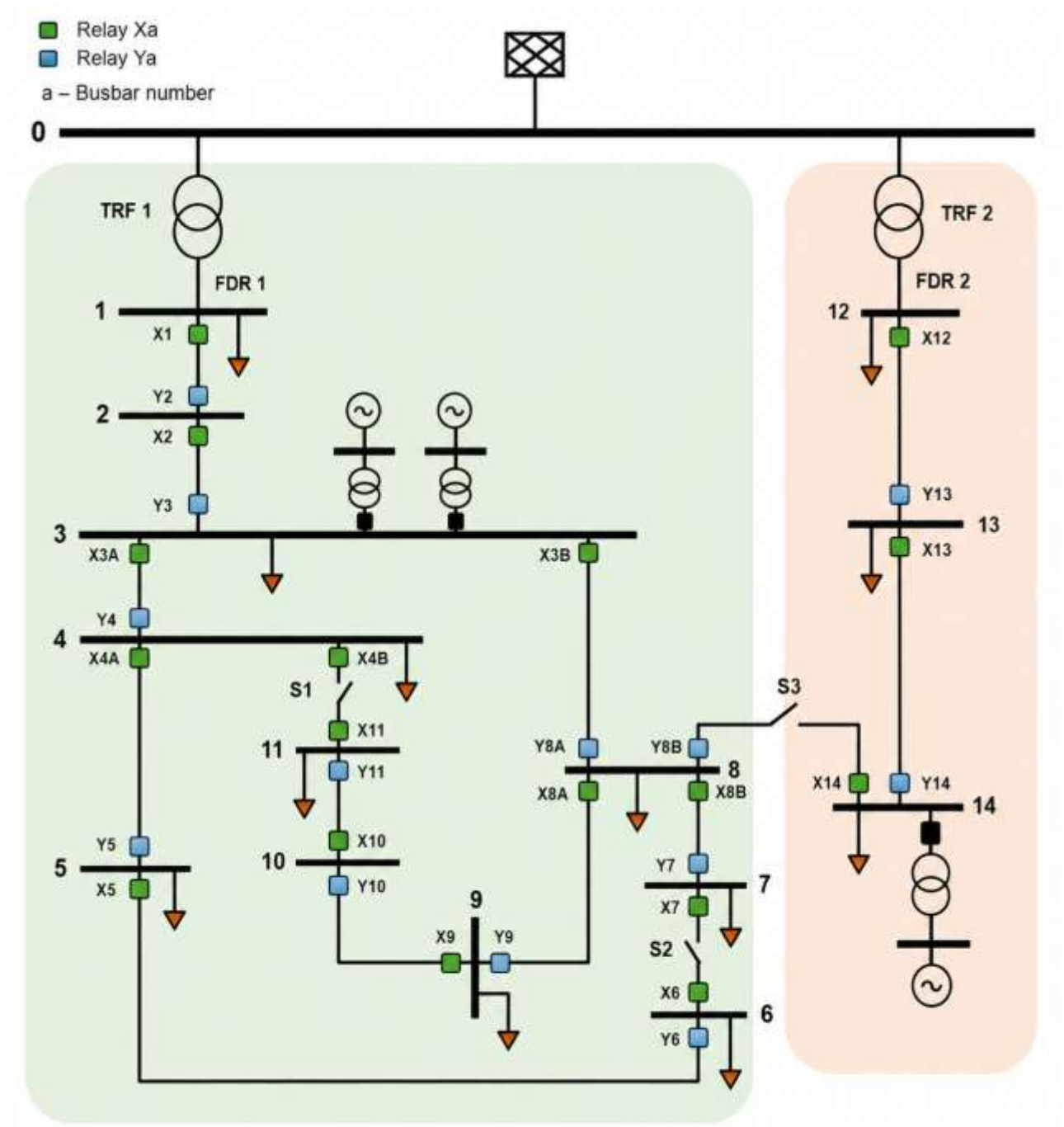


Fig. 5. Relay location on the tested CIGRE MV/LV Test System

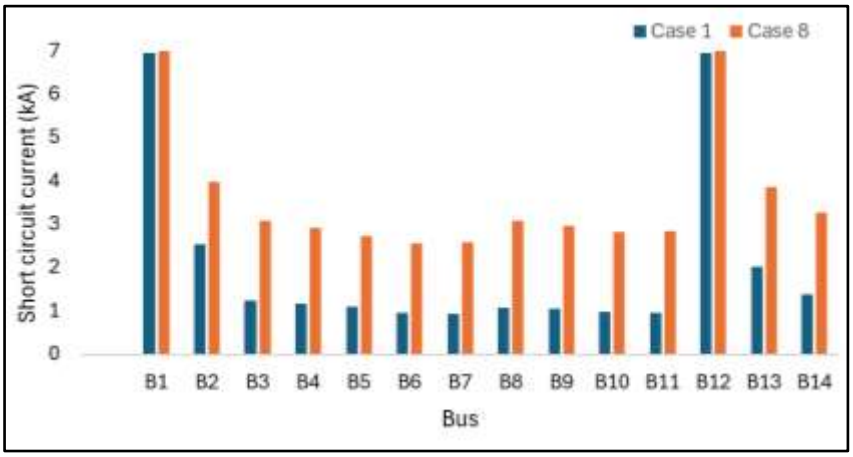


Fig. 6. Three-phase short-circuit

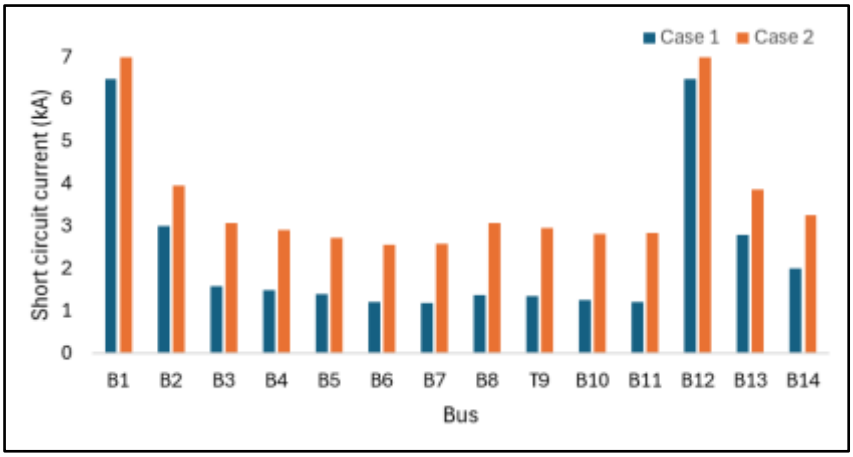


Fig. 7. Single-phase to ground short circuit

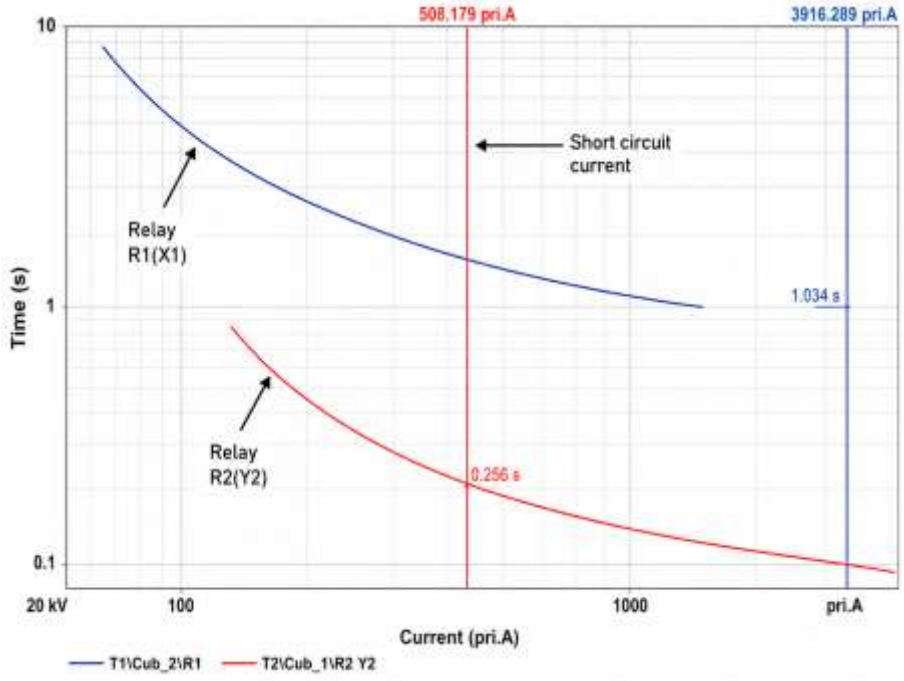


Fig. 8. Grid-connected single-phase-to-ground fault between X1 and Y2

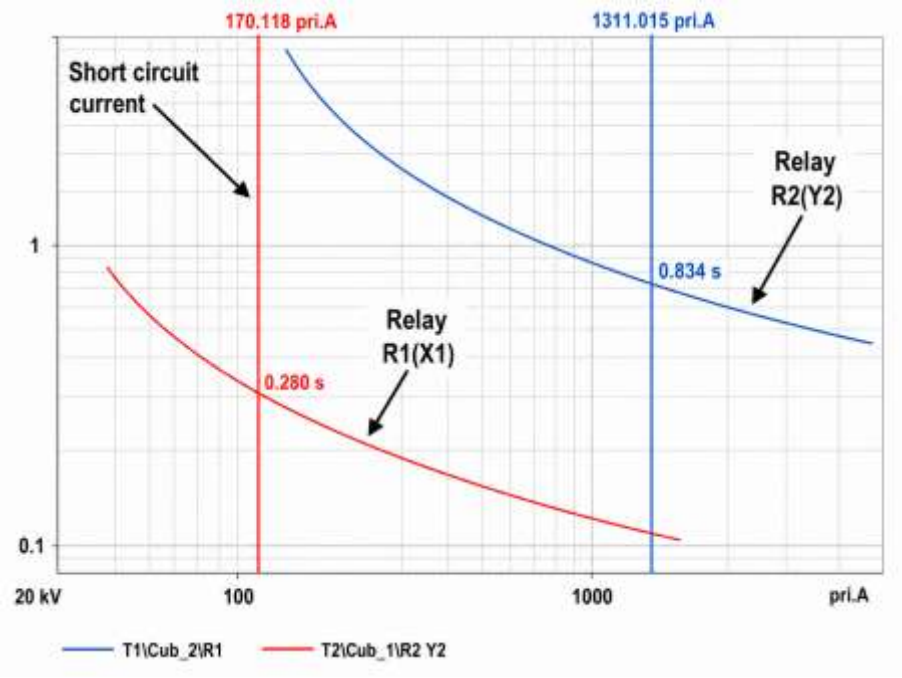


Fig. 9. Islanded single-phase-to-ground fault between X1 and Y2

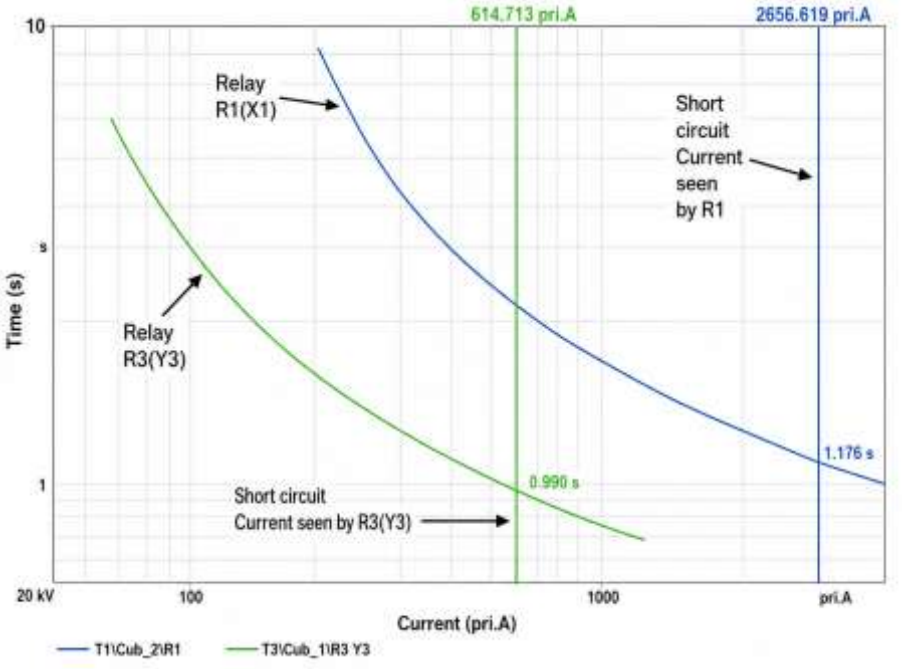


Fig. 10. Grid-connected single-phase-to-ground fault at Bus 2

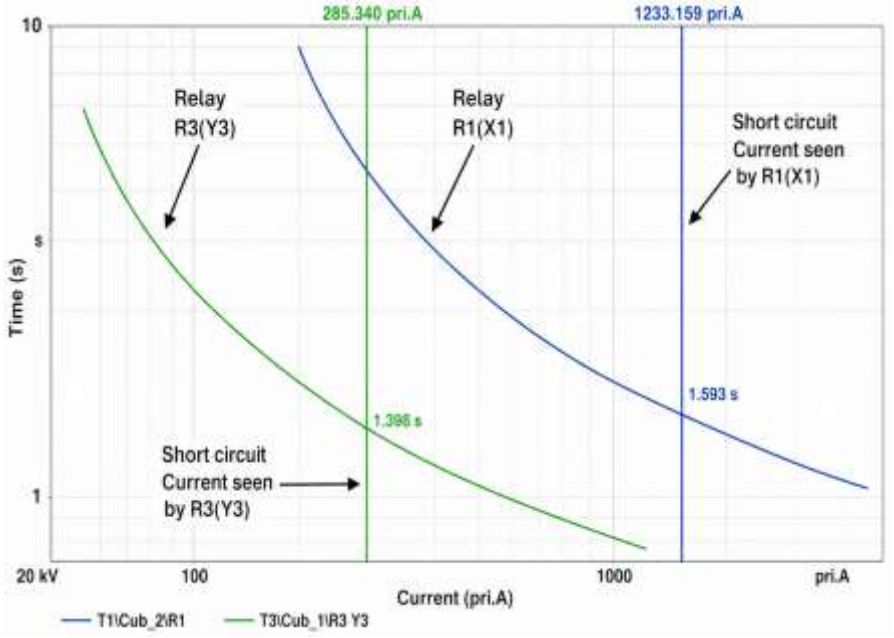


Fig. 11. Islanded single-phase-to-ground fault at Bus 2

VI. Results and Discussion

The proposed directional overcurrent relay coordination framework was evaluated using the CIGRE MV/LV Test System under grid-connected and islanded operating modes. The assessment focuses on the ability of the coordinated directional overcurrent relay (DOCR) scheme to maintain selectivity, directional discrimination, and acceptable fault-clearing performance under different network configurations. The results include short-circuit current magnitudes at the network buses and relay time-current characteristics for single-phase-to-ground faults applied at the midpoint of Line 1–2 and at Bus 2.

Fig. 6 presents the magnitudes of the three-phase short-circuit currents at all buses under grid-connected operating conditions for Cases 1 and 8. The results show that the highest fault-current levels occur at buses close to the main supply points, particularly Bus 1 and Bus 12. This is expected because these buses are electrically closer to the upstream grid sources and therefore experience stronger fault-current contributions. In contrast, buses located farther from the supply points experience lower short-circuit currents due to feeder impedance and network distance. The comparison between Cases 1 and 8 also shows that the interconnected topology generally increases the available fault current at several buses. This confirms that network configuration directly influences fault-current magnitude and must be considered when selecting relay pickup settings, CT ratios, and time-dial settings.

Fig. 7 shows the single-phase-to-ground short-circuit current magnitudes at all buses under grid-connected operation. Similar to the three-phase fault results, the single-phase-to-ground fault current varies across the network depending on the bus location and operating topology. The highest values are again observed near the main grid supply buses, while lower values occur at electrically remote locations. The comparison between the two operating cases shows that the interconnected configuration changes the short-circuit level at several buses, indicating that the relay settings must remain dependable under both maximum and minimum fault-current conditions. These results justify the use of directional overcurrent protection, since both the magnitude and possible direction of the fault current may change with changes in network topology.

Fig. 8 presents the relay time-current characteristics for a grid-connected single-phase-to-ground fault applied between relays X1 and Y2 on Line 1–2. The fault current seen by relay Y2 is approximately 508.179 A, and the relay operates in about 0.256 s. Relay X1 sees a higher current of approximately 3916.289 A and operates in about 1.034 s. Since Y2 is the relay closest to the fault, it operates as the primary protection, while X1 provides backup protection. The difference between the operating times exceeds the selected 0.3 s coordination margin, confirming that proper grading is maintained between the primary and backup relays. This result demonstrates selective fault clearing in grid-connected operation.

Fig. 9 shows the relay characteristics for the same single-phase-to-ground fault between X1 and Y2 under islanded operation. In this case, the available fault current is reduced because the network is no longer strongly supported by the main grid. Relay R1(X1) operates at approximately 0.280 s for a fault current of about 170.118 A, while relay R2(Y2) operates at approximately 0.834 s for a fault current of about 1311.015 A. Although the fault-

current magnitude is lower than in the grid-connected case, the relay pair still operates selectively and maintains the required coordination interval. This confirms that the proposed settings remain effective even under islanded conditions, where reduced fault current can make protection operation more challenging.

Fig. 10 illustrates the grid-connected single-phase-to-ground fault at Bus 2. In this case, relays R3(Y3) and R1(X1) respond according to their directional settings and measured fault-current contributions. Relay R3(Y3) sees a fault current of approximately 614.713 A and operates in about 0.990 s, while relay R1(X1) sees approximately 2656.619 A and operates in about 1.176 s. The results indicate that the relays correctly identify the fault direction and operate within the expected time-current characteristic region. The operating sequence also confirms that the protection system can discriminate between line faults and busbar faults while maintaining coordinated operation.

Fig. 11 presents the islanded single-phase-to-ground fault at Bus 2. Under this condition, the available fault current is further reduced compared with the grid-connected case. Relay R3(Y3) sees approximately 285.340 A and operates in about 1.398 s, while relay R1(X1) sees approximately 1233.159 A and operates in about 1.593 s. Longer operating times are expected because islanded operation reduces the available short-circuit current. However, both relays still detect the fault and operate within the required protection sequence. This confirms that the DOCR scheme remains dependable under reduced-current islanded operation.

Overall, Figs. 6 and 7 demonstrate that short-circuit current levels vary significantly with bus location, fault type, and network topology. Figs. 8 to 11 further confirm that the coordinated DOCR scheme can maintain correct relay operation for both line and busbar faults under grid-connected and islanded modes. The results show that the relay closest to the fault operates first, while the backup relay operates after a sufficient grading interval. Therefore, the proposed protection framework improves selectivity, avoids unnecessary tripping of healthy feeders, and maintains dependable operation under bidirectional power-flow conditions. The results also support the clearing-time ranges reported in the abstract and confirm the suitability of the proposed methodology for designing and validating directional overcurrent protection schemes in modern distribution networks.

VII. Conclusions and Future Work

The rapid evolution of modern electrical distribution systems, driven by the integration of distributed generation and renewable energy sources, has introduced significant challenges to traditional protection schemes designed for radial networks with unidirectional power flow. These changes result in bidirectional fault currents and varying short-circuit levels, which can compromise the reliability and coordination of conventional non-directional overcurrent protection systems. This study reviewed the principles and operational characteristics of Directional Overcurrent Protection Systems (DOCRs) and highlighted their importance in improving fault detection and selectivity in modern distribution networks.

The analysis demonstrated that directional overcurrent relays provide a more reliable protection approach for networks with distributed generation by considering both the magnitude and direction of fault currents. The findings confirm that properly coordinated DOCR schemes can significantly improve protection reliability, maintain system stability, and ensure selective fault isolation in increasingly complex distribution networks. Future work may focus on adaptive, intelligent protection strategies that leverage real-time system data to further enhance the resilience and efficiency of power distribution systems.

The approach outlined in this paper relies on theoretical analysis and offline software-based validation for the design of directional overcurrent protection systems. Therefore, the findings should be interpreted within the scope of the selected CIGRE MV/LV Test System and the operating scenarios considered. Although this benchmark network provides a standard, reproducible platform for protection studies involving distributed generation, further validation in larger, more complex distribution networks is required to assess the scalability of the proposed framework. In addition, the present validation focuses on single-phase-to-ground faults, which are common in distribution systems and provide a practical basis for evaluating directional discrimination and relay coordination. Future work should extend the analysis to three-phase, phase-to-phase, and double-line-to-ground faults to evaluate the framework under more severe and diverse fault conditions. Furthermore, while DIgSILENT PowerFactory provides an effective offline simulation platform, real-time digital simulation and hardware-in-the-loop testing should be incorporated to verify the practical performance of relays. Finally, adaptive and AI-based optimization methods, such as PSO or machine-learning-based relay setting approaches, may be investigated to dynamically update relay settings and coordination margins under changing network topologies, distributed-generation penetration levels, and islanded operating conditions.

Acknowledgements

The authors express their gratitude to the Cape Peninsula University of Technology (CPUT) for providing the facilities necessary to conduct this research at the Centre for Substation Automation and Energy Management Systems (CSAEMS) laboratory. This work was partially supported by the National Research Foundation (NRF) Thuthuka Grant (No. 138177) as well

as funding from the ESKOM Tertiary Education Support Programme (TESP).

Conflict of Interest

The authors declare no conflict of interest in the publication process of the research article.

Author Contributions

Sikho Ntshiba: contributed to the investigation, data collection, data analysis, and the preparation of the original draft of the manuscript.

Senthil Krishnamurthy: responsible for the conceptualization of the study, supervision of the research process, as well as the review, editing, and further investigation of the draft.

Sinawo Nomandela: also contributed to the investigation, simulation, editing, review, and documentation of the final draft.

All authors have reviewed and approved the final version of the manuscript for submission and publication in the journal.

References

[1] F. Alasali *et al.*, "Highly Sensitive Adaptive Protection for EV-Integrated Distribution Networks," *Int. Trans. Electr. Energy Syst.*, vol. 14129, no. 1, 2026, doi: 10.1155/etep/3336378.

[2] K. Sarwagya, P. K. Nayak, and S. Ranjan, "Adaptive coordination of directional overcurrent relays for meshed distribution networks with distributed generations using dragonfly algorithm," *Electr. Eng.*, vol. 105, no. 6, pp. 3511–3532, 2023, doi: 10.1007/s00202-023-01905-4.

[3] T. E. Sati, M. A. Azzouz, and M. F. Shaaban, "Harmonic Dual-Setting Directional Overcurrent Protection for Inverter-Based Islanded Microgrids," *IEEE Access*, vol. 11, pp. 34630–34642, 2023, doi: 10.1109/ACCESS.2023.3264842.

[4] S. Ntshiba and S. Krishnamurthy, "Digital Implementation of an Auto-Reclose Protection Scheme for a Distribution System," *30th South. African Univ. Power Eng. Conf.*, pp. 1–6, 2022.

[5] P. Naveen and P. Jena, "Directional Overcurrent Relays Coordination Scheme for Protection of Microgrid," *Proc. 2020 IEEE 1st Int. Conf. Smart Technol. Power, Energy Control*, 2020, doi: 10.1109/STPEC49749.2020.9297699.

[6] P. So, M. Pujiantara, A. Priyadi, and C. R. Yin, "Adaptive Protection Scheme for Optimal Relay Coordination in Tboung Khmum Radial Distribution System Using an Adaptive Modified Firefly Algorithm," *Proc. - Int. Semin. Intell. Technol. its Appl.*, no. 2025, pp. 112–117, 2025, doi: 10.1109/ISITIA66279.2025.11137477.

[7] L. Mcunukelwa and S. Nomandela, "Systematic Development and Testing of an Overcurrent Protection-based Power Redirection Technique for an Electrical Distribution System," in *2025 33rd Southern African Universities Power Engineering Conference (SAUPEC)*, IEEE, 2025, pp. 1–6. doi: 10.1109/SAUPEC65723.2025.10944356.

[8] S. I. Gkavanoudis *et al.*, "Protection philosophy in low short-circuit capacity distribution grids with high penetration of converter-interfaced distributed renewable energy sources," *IET Gener. Transm. Distrib.*, vol. 14, no. 22, pp. 4978–4988, 2020, doi: 10.1049/iet-gtd.2020.0714.

[9] C. A. Plet, M. Graovac, T. C. Green, and R. Iravani, "Fault response of grid-connected inverter dominated networks," *IEEE PES Gen. Meet. PES 2010*, pp. 1–8, 2010, doi: 10.1109/PES.2010.5589981.

[10] R. Aljarrah, H. Marzooghi, J. Yu, and V. Terzija, "Sensitivity analysis of transient short circuit current response to the penetration level of non-synchronous generation," *Int. J. Electr. Power Energy Syst.*, vol. 125, 2021, doi: 10.1016/j.ijepes.2020.106556.

[11] A. Traupmann and T. Kienberger, "Test grids for the integration of RES-A contribution for the european context," *Energies*, vol. 13, no. 20, 2020, doi: 10.3390/en13205431.

[12] M. Saber, F. M. A. Ghali, and E. E. A. Elzahab, "The effect of DG penetration on short circuit currents level," in *Intl Conf on Advanced Control Circuits Systems and Conf on New Paradigms in Electronics and Information Technology*, 2017, pp. 291–296. doi: 10.1109/ACCS-PEIT.2017.8303054.

[13] J. M. Maza-Ortega, F. J. Zarco-Soto, S. Gkavanoudis, D. Tampakis, and C. Demoulias, "A short communication to define the overcurrent protection system of the CIGRE European benchmark distribution networks for RES penetration studies," *Electr. Eng.*, vol. 104, no. 3, pp. 1331–1336, 2022, doi: 10.1007/s00202-021-01386-3.

[14] L. N. H. Pham, R. Wagle, and F. Gonzalez-Longatt, "Concise Definition of the Overcurrent Protection System for CIGRE European Medium Voltage Benchmark Network," in *IEEE PES Conference on Innovative Smart Grid Technologies - Middle East (ISGT Middle East) Proceedings*, IEEE, 2023, pp. 1–5. doi: 10.1109/ISGTMiddleEast56437.2023.10078621.

[15] M. Biller, J. Jaeger, I. Mladenovic, C. Schacherer, D. Wolter, and M. Stoetzel, "Protection systems in distribution grids with variable short-circuit conditions," in *International Conference on Development in Power System Protection*, 2016, pp. 1–5. doi: 10.1049/cp.2016.0086.

[16] L. N. H. Pham, V. Rosero-Morillo, and F. Gonzalez-Longatt, "Directional Overcurrent Protection Design for Distribution Network: CIGRE European Medium-Voltage Benchmark Network †," *Eng. Proc.*, vol. 77, no. 1, 2024, doi: 10.3390/engproc2024077026.

[17] IEC 60255, "Measuring relays and protection equipment." 2009.

[18] IEEE C37.112, "IEEE Std C37.112. Standard for Inverse- Time Characteristics Equations for Overcurrent Relays." 2018.

[19] IEEE Std C37.110, "IEEE Guide for application of current transformers used for protection relaying purposes." 1996.

[20] Cutler-Hammer, *Fundamentals of Electrical Distribution*. Milwaukee: Cutler-Hammer and Eaton Corp, 1999.

[21] D. Muhammad Soomro, A. Hasan Tawafan, and F. Ibrahim Jabbar, "Methods in Single Phase to Ground Faults on Power Distribution Systems," *J. Eng. Appl. Sci.*, vol. 14, no. 7, pp. 10058–10066, 2019, doi: 10.36478/jeasci.2019.10058.10066.

[22] K. Strunz, *Benchmark Systems for Network Integration of Renewable and Distributed Energy Resources.* Paris, France: CIGRE, 2014.